

Pullout capacity of shallow inclined anchor in anisotropic and nonhomogeneous undrained clay

Paramita Bhattacharya*

Department of Civil Engineering, Indian Institute of Technology Kharagpur, Kharagpur-721302, India

(Received August 18, 2016, Revised May 1, 2017, Accepted May 15, 2017)

Abstract. This study aimed to find out the pullout capacity of inclined strip anchor plate embedded in anisotropic and nonhomogeneous fully saturated cohesive soil in undrained condition. The ultimate pullout load has been found out by using numerical lower bound finite element analysis with linear programming. The undrained pullout capacity of anchor plate of width B is determined for different embedment ratios (H/B) varying from 3 to 7 and various inclination of anchor plates ranging from 0° to 90° with an interval of 15° . In case of anisotropic fully saturated clay the variation of cohesion with direction has been considered by varying the ratio of the cohesion along vertical direction (c_v) to the cohesion along horizontal direction (c_h). In case of nonhomogeneous clay the cohesion of the undrained clay has been considered to be increased with depth below ground surface keeping $c_v/c_h=1$. The results are presented in terms of pullout capacity factor ($F_{c0}=p_u/c_H$) where p_u is the ultimate pullout stress along the anchor plate at failure and c_H is the cohesion in horizontal direction at the level of the middle point of the anchor plate. It is observed that the pullout capacity factor increases with an increase in anisotropic cohesion ratio (c_v/c_h) whereas the pullout capacity factor decreases with an increase in undrained cohesion of the soil with depth.

Keywords: inclined anchor plate; anisotropic clay; nonhomogeneous clay; limit analysis; pullout capacity

1. Introduction

Anchors are frequently used as tensile element for foundation subjected to pullout loading such as dry-docks, transmission towers, sheet-piles, buried pipe lines under water. A large number of research investigations are found in literature dealing with the pullout capacity of anchor plates embedded either in clay or sand. For example, Rowe and Davis (1982), Desai *et al.* (1986), Song *et al.* (2008), Wang *et al.* (2010), Yu *et al.* (2011), Chen *et al.* (2013), Niroumand and Kassim (2014a, b, c), Tho *et al.* (2014), Demir and Ok (2015) and Keskin (2015) performed the displacement based elasto-plastic finite element analysis, Basudhar and Singh (1994), Merifield *et al.* (2001), Merifield *et al.* (2005), Khatri and Kumar (2009), Yu *et al.* (2014), Yu *et al.* (2015), Bhattacharya (2016), Bhattacharya and Roy (2016) studied the pullout capacity of the anchor plates by using limit analysis (either lower or upper bound limit analysis or both). A few small scale 1-g model tests, field tests and centrifuge tests are also reported in literature by Meyerhof (1973), Das and Seeley (1975), Ovesen (1981), Dickin and Leung (1983), Desai *et al.* (1986),

*Corresponding author, Assistant Professor, E-mail: paramita@civil.iitkgp.ernet.in

Sutherland (1988), Rao and Prasad (1992), Ilamparuthi and Muthukrsihnaiah (1999), Niroumand and Kassim (2014a, b, c), Demir and Ok (2015) and Keskin (2015). Depending upon its application and types of loading anchor can be placed at an inclination. Among the works reported herein Merifield *et al.* (2005) studied the pullout capacity of inclined anchor embedded in uniform clay. Yu *et al.* (2011) determined the pullout capacity of inclined anchor plate considering linear variation of cohesion of clay by using the AFENA finite element software where the stress-strain response of clay mass under undrained condition was simulated by the elasto-plastic model based on the Tresca failure criterion. In their study Yu *et al.* (2011) investigated the effect of non-homogeneity with a linear variation of cohesion with depth only for horizontal and vertical anchor plates. Yu *et al.* (2015) evaluated the undrained pullout capacity of deeply embedded inclined strip anchor plate in clay with a linear variation of shear strength with depth by block set mechanism and numerical upper and lower bound limit analyses.

In reality the strength parameters of soils are anisotropic. Although a lot of research investigations are carried out to study the bearing capacity of footings and stability of slopes in anisotropic soil (Lo 1965, Davis and Christian 1971, Yu and Sloan 1994, Nian *et al.* 2008, Jha 2016) no research works are carried out to determine the pullout capacity of anchor plates (horizontal, inclined or vertical anchor plates) embedded in anisotropic fully saturated clays. The effect of non-homogeneity of shear strength parameters in normally and slightly over consolidated clay on pullout capacity of horizontal and vertical anchor plate were investigated by Yu *et al.* (2011) following elasto-plastic FE method. Except the work reported by Yu *et al.* (2011) based on empirical solutions suggested by Das and Puri (1989) no rigorous numerical investigation considering vented/immediate breakaway condition is found in literature to study pullout capacity of shallow inclined strip anchor plate (other than horizontal and vertical plates) in nonhomogeneous clay. This is the motivation to carry out the present research work. Since numerical lower bound limit analysis provides the safe estimate of the ultimate load for bearing capacity problems of footings (Lyamin and Sloan 2002, Kumar and Khatri 2008) and stability problems of anchor plates (Merifield *et al.* 2001, Merifield *et al.* 2005, Yu *et al.* 2015, Bhattacharya 2016) the present research investigations have been carried out by using numerical lower bound limit analysis with finite elements and linear programming. The ultimate undrained pullout capacity of the anchor plates at different orientations have been determined for different embedment ratio (H/B), different anisotropic cohesion ratio (c_v/c_h), and different degree of non-homogeneity of fully saturated weightless cohesive soils. The failure patterns are studied for a few cases. Comparisons of the present results are also done with available results in literature.

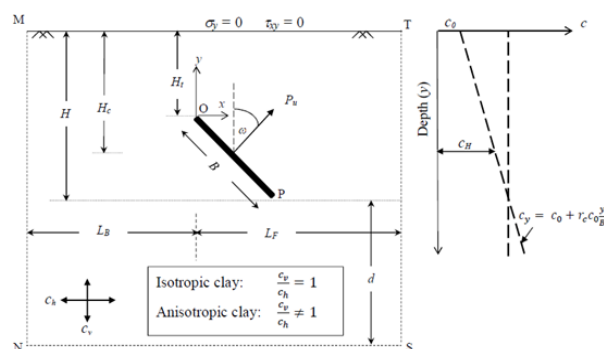


Fig. 1 Schematic diagram of the problem

2. Problem definition

A strip plate anchor, of width B , is embedded with an inclination of ω with horizontal axis (-ve x -axis) in fully saturated clay deposit. A schematic diagram of the chosen problem has been shown in Fig. 1. The vertical distances of the top and bottom edges of the anchor plate measured from the horizontal ground surface are H_t and H_b , respectively, whereas the distance between the horizontal ground surface and the middle of the anchor plate is H_c . The thickness of the plate is negligible in comparison to its width (B). It is required to determine the maximum pullout resistance (P_u) offered by the anchor plate at different orientation varying from 0° to 90° with an interval of 15° where the direction of pulling out is perpendicular to the plate. The cohesions on the vertical and horizontal planes are c_v and c_h , respectively. The undrained pullout resistance of the inclined plate anchor has been determined for (i) fully saturated anisotropic clay where cohesion varies with directions for c_v/c_h equal to 0.5 to 2 with 0.5 intervals following the literature (Pan and Dias 2016, Wang and Yu 2014 and Yu and Sloan 1994) and (ii) fully saturated nonhomogeneous clay with a linear variation of undrained cohesion with depth considering $c_v/c_h=1$. The analysis of anchor plate can be carried out either considering immediate breakaway condition or fully bonded condition. In case of immediate breakaway condition the bottom surface of the anchor plate cannot offer any resistance against pullout whereas some amount of resistance always being offered by the soil-bottom interface surface of the anchor plate against pullout. The magnitude of the suction or adhesion force developed along the soil-bottom interface of the anchor plate is highly uncertain. Therefore the immediate breakaway condition is assumed for the present analysis which may provide conservative but safe estimate of the ultimate pullout load.

2.1 Domain, finite element mesh and stress boundary conditions

A rectangular domain MNST representing a fully saturated cohesive soil domain, as shown in Fig. 1, is chosen for the present analysis. An anchor is positioned along OP with an inclination of ω with respect to the horizontal axis in the soil domain. The left and right sides vertical boundaries (MN and ST) and the bottom boundary (NS) of the domain MNST must be kept at sufficient distances away from the anchor plate such that (i) none of the yielded element can touch the boundaries and (ii) any change in the size of the domain could not cause any change in the magnitude of the ultimate pullout load. The one hand, the horizontal distance (L_B) between the upper/left edge of the anchor plate and the vertical boundary MN is varied between $6B$ to $16B$ whereas the distance between the bottom/right edge of the anchor plate and the right vertical boundary ST is varied between $9B$ to $21B$. On the other hand, the vertical distance between the bottom edge of the anchor plate and the bottom boundary of the domain (NS) is kept between $9B$ to $16B$. The stress boundary conditions are presented in Fig. 1. The normal (σ_y) and shear (τ_{xy}) stresses along the stress free horizontal ground surface are considered to be zero.

$$\sigma_y = 0 \text{ and } \tau_{xy} = 0 \quad (1a)$$

No other boundary conditions are imposed on the two verticals and the bottom boundaries of the domain. Since an immediate breakaway condition has been imposed behind the anchor plate and the adjoining soil mass, therefore, normal stress (σ_n) and shear stress (τ) acting along the back surface of the anchor plate becomes simply equal to zero. On the other hand, along the interface between the front face of the anchor plate and adjoining soil mass, the following stress boundary condition is specified

$$|\tau| \leq c_\omega \quad (1b)$$

where τ and c_ω is the interface shear stress and interface cohesion, respectively. Here the interface plane makes an angle ω with respect to $-ve$ x -axis or $\pi-\omega$ with respect to the positive x -axis. For the plane of anchor plate i.e., OP, $\theta=\pi-\omega$.

Normal and shear stresses acting on any plane inclined at an angle β with horizontal plane can be expressed in terms of unknown nodal stresses by using following equations

$$\sigma_n = \sigma_x \sin^2 \beta + \sigma_y \cos^2 \beta - \tau_{xy} \sin 2\beta \quad (1c)$$

$$\tau = -\frac{1}{2} \sigma_x \sin 2\beta + \frac{1}{2} \sigma_y \sin 2\beta + \tau_{xy} \cos 2\beta \quad (1d)$$

In the present numerical analysis both isotropic and anisotropic cohesive soils are considered. In case of anisotropic cohesive soil, the cohesion on any plane with a direction of θ with respect to $+ve$ x -direction can be expressed by following equation based on Lo (1965)

$$c_\theta = c_h + (c_v - c_h) \sin^2 \theta \quad (1e)$$

where c_v and c_h are cohesions along vertical and horizontal planes, respectively.

The shear strength developed on any plane with a direction of θ can be represented as

$$s = c_\theta - \sigma_n \tan \phi_u = c_h + (c_v - c_h) \sin^2 \theta - \sigma_n \tan \phi_u \quad (1f)$$

It should be noted that for undrained cohesive soil $\phi_u = 0$.

The chosen domain is discretized into a number of three noded triangular elements. The sizes of the elements are chosen in such a way that sizes are decreased towards the edges of the anchor plate. Typical finite element meshes for $H/B = 5$, $\omega = 30^\circ$ and 60° are shown in Fig. 2 where N , E and D_c represents the total number of nodes, elements and stress discontinuities, respectively. The values of N , E and D_c increases with increase in values of H/B and ω .

3. Analysis

3.1 Numerical formulation for lower bound limit analysis with finite elements

Present numerical analysis has been carried out by employing lower bound finite element limit analysis with linear programming in plane strain condition as proposed by Sloan (1988) and Yu and Sloan (1994). The nodal stresses, say σ_x , σ_y , and τ_{xy} , are considered as basic unknown variables. In lower bound limit analysis the following element equilibrium conditions are satisfied everywhere in the domain

$$\frac{\partial \sigma_x}{\partial x} + \frac{\partial \tau_{xy}}{\partial y} = 0 \quad (2a)$$

$$\frac{\partial \tau_{xy}}{\partial x} + \frac{\partial \sigma_y}{\partial y} = \gamma \quad (2b)$$

where γ is the unit weight of the soil mass which is considered to be zero in the present analysis with weightless cohesive soil.

Statically admissible stress discontinuities are considered along all the common edges shared by any two adjacent elements. In this process continuity of shear and normal stresses are maintained at the two nodes being part of a common edge and with same coordinates whereas there is a discontinuity of tangential stresses along the same edge. The stress boundary conditions mentioned in Eq. (1a) are imposed along the stress free horizontal ground surface. Thus, the element equilibrium condition, discontinuity equilibrium and stress boundary condition on ground surface have formed the equality constraints.

In order to derive the modified Mohr-Coulomb failure criterion for anisotropic soil it is necessary to determine orientation of the critical plane at each point in the soil domain for which $\frac{d(\tau-s)}{d\theta} = 0$. For undrained cohesive soil $\phi_u=0$ and therefore the orientation of the critical plane can be obtained as: $\tan 2\theta = \frac{\sigma_y - \sigma_x}{c_v - c_h - 2\tau_{xy}}$.

The following modified Mohr-Coulomb strength criterion derived considering the directional strength variation for anisotropic cohesive soil presented in expression (3a) has been adopted

$$F = (\sigma_y - \sigma_x - 2\tau_{xy} \tan \phi_u)^2 + (c_v - c_h + 2\tau_{xy} - \sigma_x \tan \phi_u + \sigma_y \tan \phi_u)^2 - (c_v + c_h - \sigma_x \tan \phi_u - \sigma_y \tan \phi_u)^2 = 0 \tag{3a}$$

where undrained soil friction angle for saturated clay $\phi_u = 0$.

In order to ensure linear programming problem due to its simplicity, the modified Mohr-Coulomb yield criterion has been linearized following Yu and Sloan (1994) as shown below

$$A_k \sigma_x + B_k \sigma_y + C_k \tau_{xy} \leq D_k \quad k = 1, 2, \dots, p \tag{3b}$$

where, $A_k = -\cos\left(\frac{2\pi k}{p}\right) - \tan \phi_u \sin\left(\frac{2\pi k}{p}\right) + \tan \phi_u \cos\left(\frac{\pi}{p}\right)$;

$$B_k = \cos\left(\frac{2\pi k}{p}\right) + \tan \phi_u \sin\left(\frac{2\pi k}{p}\right) + \tan \phi_u \cos\left(\frac{\pi}{p}\right); C_k = -2 \tan \phi_u \cos\left(\frac{2\pi k}{p}\right) + 2 \sin\left(\frac{2\pi k}{p}\right)$$

$$D_k = (c_h + c_v) \cos\left(\frac{\pi}{p}\right) + (c_h - c_v) \sin\left(\frac{2\pi k}{p}\right)$$

The yield criterion (3b) along with the interface condition between top surface of the anchor plate and its surrounding soil mass i.e., inequality condition (1b) have constituted a set of inequality constrains. The magnitude of the ultimate pullout load per unit length in plane strain condition has been derived by integrating numerically the normal stresses acting along the soil-front or top face of the anchor plate as presented below

$$P_u = \int_B^{\text{Front or top surface}} \sigma_n ds = -\{f_{obj}\}^T \{\sigma\} \tag{4}$$

where σ_n is the normal stress acting over the width B of the plate and $\{\sigma\} = \{\sigma_x \quad \sigma_y \quad \tau_{xy}\}^T$ and $\{f_{obj}\}^T$ is the coefficient matrix of the objective function.

Thus, the objective function consisted of the magnitude of the collapse load per unit length (P_u) is maximized subjected to a set of equality and inequality linear constraints as shown in the following canonical form

$$\text{Maximize the objective function } -\{f_{obj}\}^T \{\sigma\} \tag{5a}$$

$$\text{Subjected to (i) equality constraints } [A_{eq}]\{\sigma\} = \{B_{eq}\} \tag{5b}$$

$$\text{(ii) inequality constraints } [A_{ineq}]\{\sigma\} \leq \{B_{ineq}\} \tag{5c}$$

The LINPROG function available in MATLAB 2013 is used to solve the linear optimization.

3.2 Definition of pullout capacity factor F_{c0}

The pullout capacity factor (F_{c0}) can be defined as the magnitude of the undrained ultimate pullout stress ($p_u = \frac{P_u}{B}$) of a strip anchor plate embedded in a fully saturated clay to the undrained cohesion in horizontal direction at the level of the middle point of the anchor plate where $c_h=c_H$. Following Eq. (6) represents the mathematical expression of pullout capacity factor

$$F_{c0} = \left(\frac{P_u}{c_H B} \right) \tag{6}$$

It is worthy to mention here that the soil is assumed to be weightless i.e., $\gamma=0$ in Eq. (6) and the pullout capacity factor ($F_{c\gamma}$) for $\gamma \neq 0$ can be determined by simply adding normalized overburden pressure ($\gamma H/c_H$) of the soil mass lying above the anchor plate to the pullout capacity factor F_{c0} .

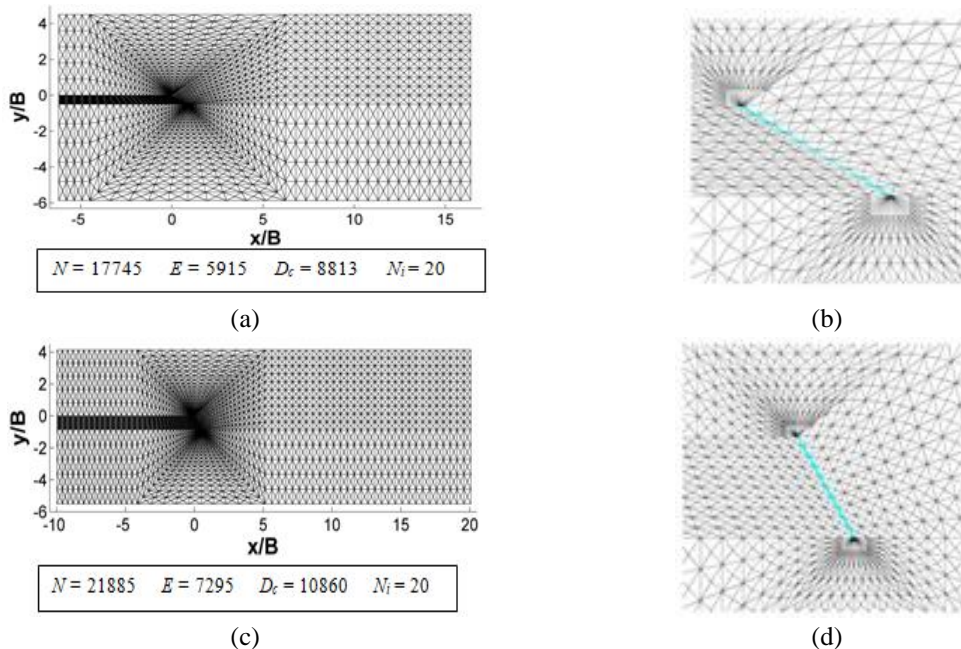


Fig. 2 Typical finite element meshes for $H/B=5$ with (a) full view for $\omega=30^\circ$, (b) zoomed view around anchor plate for $\omega=0^\circ$, (c) full view for $\omega=60^\circ$, and (d) zoomed view around anchor plate for $\omega=60^\circ$

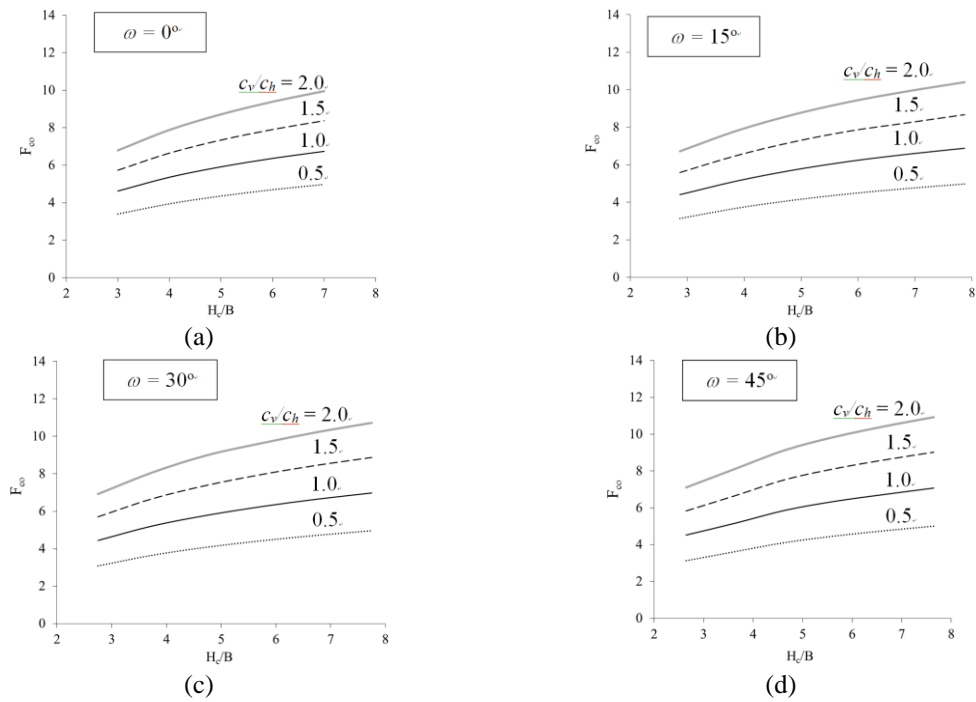


Fig. 3 Variation of F_{c0} with H_c/B for different values of c_v/c_h when (a) $\omega=0^\circ$, (b) $\omega=15^\circ$, (c) $\omega=30^\circ$, and (d) $\omega=45^\circ$

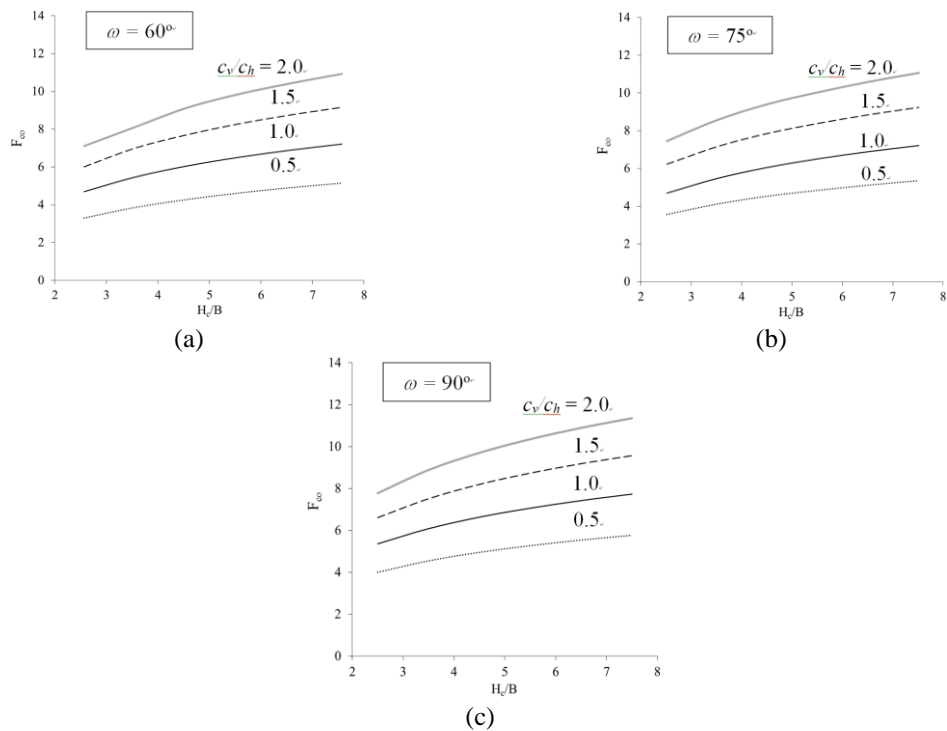
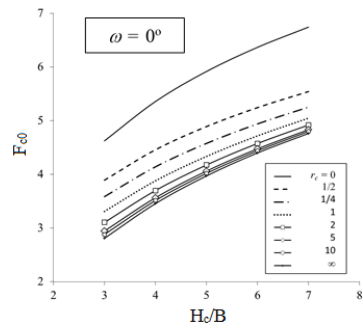
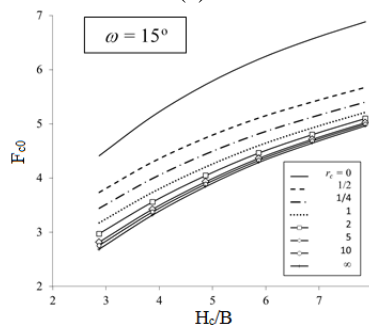


Fig. 4 Variation of F_{c0} with H_c/B for different values of c_v/c_h when (a) $\omega=60^\circ$, (b) $\omega=75^\circ$, and (c) $\omega=90^\circ$

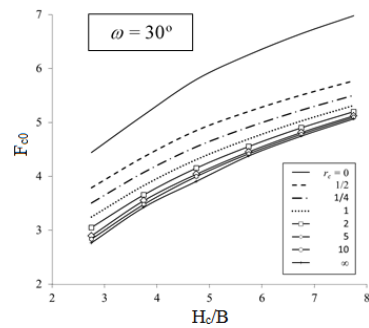


(a)

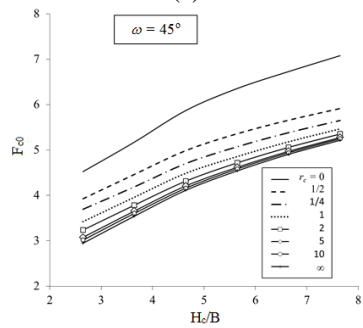


(b)

Fig. 5 Variation of F_{c0} with H_c/B for different values of r_c when (a) $\omega=0^\circ$ and (b) $\omega=15^\circ$



(a)



(b)

Fig. 6 Variation of F_{c0} with H_c/B for different values of r_c when (a) $\omega=30^\circ$ and (b) $\omega=45^\circ$

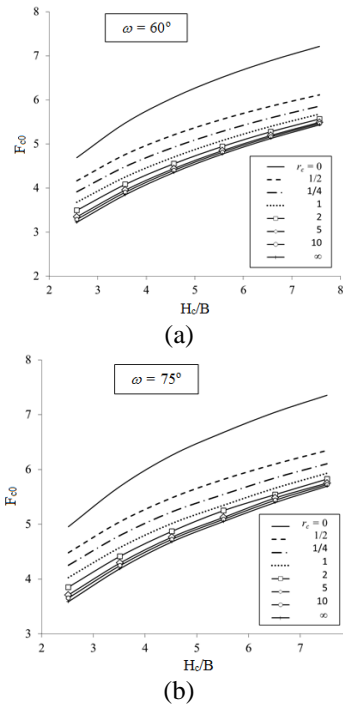


Fig. 7 Variation of F_{c0} with H_c/B for different values of r_c when (a) $\omega=60^\circ$ and (b) $\omega=75^\circ$

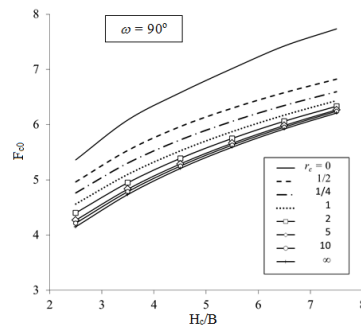


Fig. 8 Variation of F_{c0} with H_c/B for different values of r_c when $\omega=90^\circ$

4. Results and comparison

4.1 Variation of F_{c0} in anisotropic clay

Variation of the undrained pullout capacity of the inclined anchor plate for different values of embedment ratio (H_c/B), degree of anisotropy (c_v/c_h) and inclination angle of the plate (ω) has been presented in Figs. 3 and 4. The rough anchor plate has been analyzed in this case. The pullout capacity of the anchor plate has been found to be increased with an increase in the degree of anisotropy i.e., c_v/c_h . It implies that the pullout capacity of anchor plate is greatly influenced by the anisotropy in vertical direction in comparison to the anisotropy in horizontal direction. For example, the value of F_{c0} in clay with $c_v/c_h=0.5$ and 2 are approximately 0.7 times and 1.5 times

the F_{c0} value in clay with $c_v/c_h=1$ (isotropic clay), respectively, for horizontal anchor plate. However, the rate of increase in pullout capacity decreases with an increase in c_v/c_h . For example, the rate of increase of pullout capacity has been found to be approximately equal to or greater than 36% and 19% for an increase in c_v/c_h from 0.5 to 1 and 1.5 to 2.0, respectively, for $\omega=0^\circ$. The pullout capacity of the plate also increases with an increase in embedment ratio (H_c/B) and the inclination of the anchor plate.

4.2 Variation of F_{c0} in nonhomogeneous clay

It is reported in the literature that the cohesion of normally consolidated clay and slightly over consolidated clay increases linearly with the depth below ground surface (Bishop 1966). Therefore, in order to study the effect of soil non-homogeneity on the undrained pullout capacity of the inclined anchor plate the variation of the pullout capacity factor (F_{c0}) with H_c/B has been plotted considering different rate of increase in cohesion with depth.

In this context the cohesion of soil mass is assumed to increase linearly with depth measured from the ground surface (y) following Eq. (7) as shown below

$$c_y = c_0 + r_c c_0 y/B \quad (7)$$

where c_y and c_0 are the cohesion of undrained clay at depth y below the ground surface and cohesion at the ground surface, respectively, r_c is a non-dimensional number which defines the rate at which cohesion increases linearly with depth below ground surface. Therefore, c_H is the cohesion at a depth H_c from the ground surface as shown in Fig. 1. The variation of pullout capacity factor (F_{c0}) in nonhomogeneous isotropic clay with H_c/B are illustrated in Figs. 5-8 for seven different values of inclination angle (ω) of the anchor plate. It is noted in Figs. 5-8 that the pullout capacity factor (F_{c0}) decreases with an increase in the normalized rate of change in cohesion (r_c) for all combination of H_c/B and ω . In the present analysis for r_c infinity c_0 is assumed to be zero at the top surface. However very small change in F_{c0} value is observed with an increase in r_c for $r_c > 2$. Although F_{c0} has been found to decrease with an increase in r_c , the total resistance capacity against pulling out increases with an increase in r_c . This is happened because due to non-homogeneity the undrained cohesion increases with depth and hence the strength of the soil also increases.

4.3 Comparison of present lower bound solution with available works in literature

The present lower bound solution for pullout capacity of inclined anchor plate embedded in isotropic homogeneous weightless clay has been compared with available solutions provided by Merifield *et al.* (2001) for $\omega=0^\circ$ and 90° and Merifield *et al.* (2005) for $\omega=45^\circ$ by using upper and lower bounds finite element limit analysis, Yu *et al.* (2011) for $\omega=0^\circ$, 45° and 90° and Rowe and Davis (1982), Song *et al.* (2008) and Wang *et al.* (2010) for $\omega=0^\circ$ and 90° . Rowe and Davis (1982) performed elasto-plastic finite element analysis with the usage of k_4 theory. As per k_4 definition of failure the ultimate load is measured correspond to an apparent stiffness of $1/4^{\text{th}}$ of the elastic stiffness. Song *et al.* (2008) carried out elasto-plastic analysis by remeshing and interpolation techniques with small strain mode model (RITSS). Wang *et al.* (2010) conducted large deformation finite element analysis to study the uplift capacity of anchor. Yu *et al.* (2011) performed finite element analysis by using elasto-plastic finite element method with AFENA software. The comparison for isotropic, homogenous clay is presented in Fig. 9. The present

results match well with the lower bound solutions provided by Merifield *et al.* (2001) for both horizontal and vertical anchor plate, Merifield *et al.* (2005) for inclined anchor plate with $\omega=45^\circ$ and Yu *et al.* (2011). Yu *et al.* (2011) derived equations for $\omega=0^\circ$ and 90° with $R^2=0.999$ and used the empirical equations proposed by Das and Puri (1989) for square plate anchor with $\omega=45^\circ$ which were considered for the comparison.

The upper bound solutions given by Merifield *et al.* (2001) and displacement based FEA results by Song *et al.* (2008) and Wang *et al.* (2010) were always found to be on the higher side. Because of the k_4 definition of failure the ultimate pullout capacity of horizontal and vertical plate anchors reported by Rowe and Davis (1982) were found to be the lowest compared to all available results.

Although no rigorous solution has been found on pullout capacity of inclined anchor plate in nonhomogeneous clay for $0^\circ < \omega < 90^\circ$ Merifield *et al.* (2001) and Yu *et al.* (2011) reported the non-homogeneity factor (η_{rc}) of clay soil for horizontal and vertical anchor plates as defined below

$$\eta_{rc} = (F_{c0})_{c_v/c_h=1, r_c \neq 0} / (F_{c0})_{c_v/c_h=1, r_c=0} \quad (8)$$

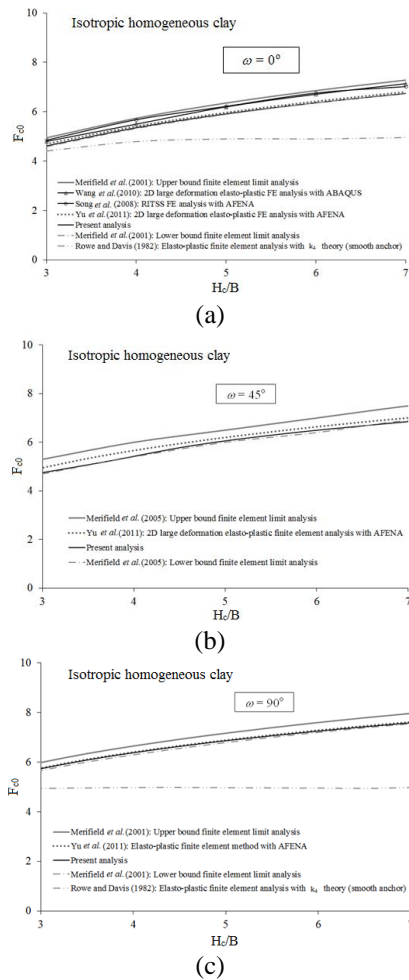


Fig. 9 Variation of F_{c0} with H_c/B for different values of r_c when (a) $\omega=0^\circ$, (b) $\omega=45^\circ$, and (c) $\omega=90^\circ$

Table 1 Comparison of present $\eta_{r_c} = (F_{c0})_{c_v/c_h=1, r_c \neq 0} / (F_{c0})_{c_v/c_h=1, r_c=0}$ values with available results in literature

ω	r_c	H/B	$\eta_{r_c} = (F_{c0})_{c_v/c_h=1, r_c \neq 0} / (F_{c0})_{c_v/c_h=1, r_c=0}$		
			Present analysis ¹	Merifield <i>et al.</i> (2001) ²	Yu <i>et al.</i> (2011) by AFENA FEA ³
0°	0.5	3	0.775	0.785* (0.789)**	0.767
		4	0.773	0.783 (0.784)	0.765
		5	0.773	0.783 (0.787)	0.771
		6	0.776	0.786 (0.802)	0.776
		7	0.779	0.814 (0.824)	0.779
	1	3	0.716	0.736 (0.739)	0.707
		4	0.724	0.736 (0.738)	0.718
		5	0.732	0.735 (0.740)	0.733
		6	0.741	0.739 (0.742)	0.743
		7	0.748	0.740 (0.766)	0.752
	2	3	0.671	-	0.665
		4	0.690	-	0.686
		5	0.705	-	0.708
		6	0.718	-	0.724
		7	0.729	-	0.735
90°	0.5	3	0.888	0.889 (0.952)	0.852
		4	0.872	0.878 (0.917)	0.843
		5	0.870	0.873 (0.889)	0.842
		6	0.864	0.868 (0.880)	0.842
		7	0.855	0.857 (0.882)	0.843
	1	3	0.851	0.852 (0.918)	0.810
		4	0.838	0.844 (0.897)	0.808
		5	0.840	0.832 (0.872)	0.813
		6	0.837	0.835 (0.833)	0.818
		7	0.831	0.831 (0.839)	0.822
	2	3	0.821	-	0.778
		4	0.813	-	0.785
		5	0.819	-	0.794
		6	0.820	-	0.803
		7	0.816	-	0.809

¹Numerical lower bound finite element limit analysis with linear programming^{2*}Numerical lower bound finite element limit analysis^{2**}Numerical upper bound finite element limit analysis³Elasto-plastic finite element analysis with finite element software AFENA

These reported η_{rc} values are compared with the η_{rc} values obtained from present lower bound limit analysis. The comparison of η_{rc} for nonhomogeneous soil are presented in Table 1 for different values of H/B for horizontal and vertical anchor plates. The present η_{rc} values match well with the results reported by Merifield *et al.* (2001) with the usage of lower bound limit analysis and Yu *et al.* (2011) with the usage of finite element software AFENA. For $\omega=0^\circ$ the present ratio becomes close to the values reported by Yu *et al.* (2011) and for $\omega=90^\circ$ the present ratio has been found to be close to the lower bound solutions of Merifield *et al.* (2001). The upper bound limit analysis provides higher value of the ratio for all cases. It is found from this comparison that the ratio of η_{rc} becomes higher for lower value of normalized rate of increase of cohesion i.e., lower value of r_c for all combination of H/B and ω .

4.4 Variation of pullout capacity ($F_{c\gamma}$) with soil over burden pressure ($\gamma H_o/c_u$)

The variation of the pullout capacity ($F_{c\gamma}$) of anchor plate with normalized overburden pressure $\gamma H_o/c_u$ has been plotted for (i) three different embedment ratio (say $H/B=3, 5$ and 7) and (ii) inclination of the anchor plate (say $\omega=0^\circ, 60^\circ, 75^\circ$ and 90°). The results are presented in Figs. 10-12. The analysis has been carried out for isotropic and homogeneous clay with $a_r=1$ and $r_c=0$ in Figs. 10(a)-(b), isotropic and non-homogeneous clay with $a_r=1$ and $r_c=1$ as shown in Figs. 10(c)-10(d) and anisotropic and homogeneous clay with $a_r=0.5-2$ and $r_c=0$ as illustrated in Figs. 11-12. In addition to the results presented in Figs. 10-12 a few more analysis has also been carried out for

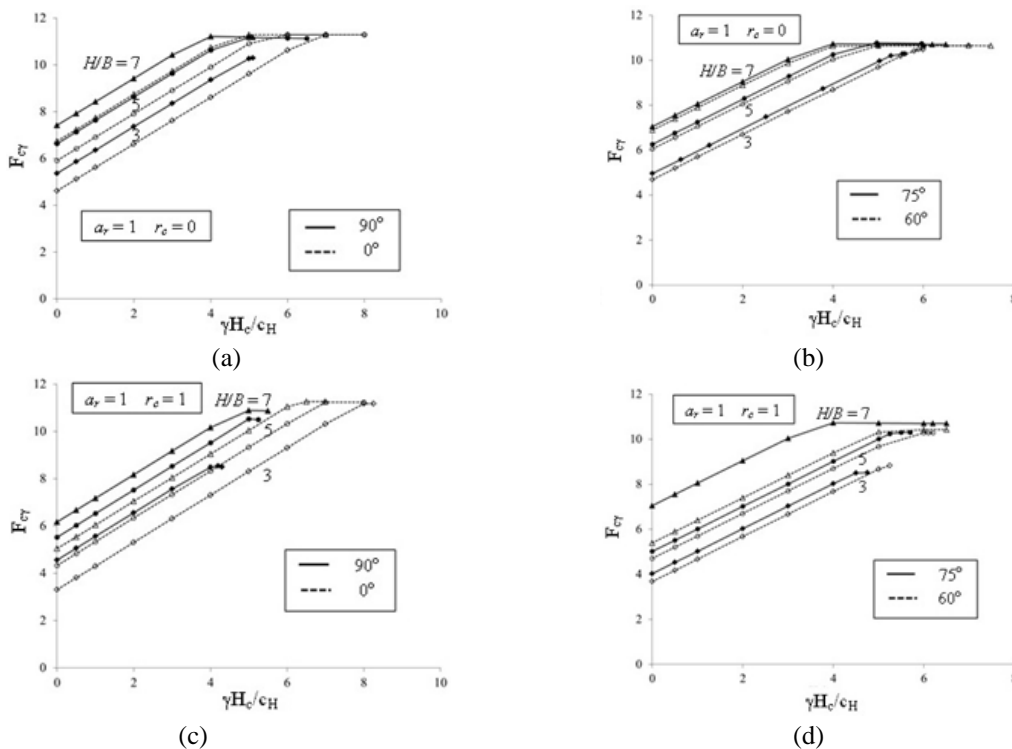


Fig. 10 Variation of $F_{c\gamma}$ with $\gamma H_o/c_u$ for isotropic clay with (a)-(b) $a_r=1$ and $r_c=0$ (homogeneous) and (c)-(d) $a_r=1$ and $r_c=1$ (non-homogeneous)

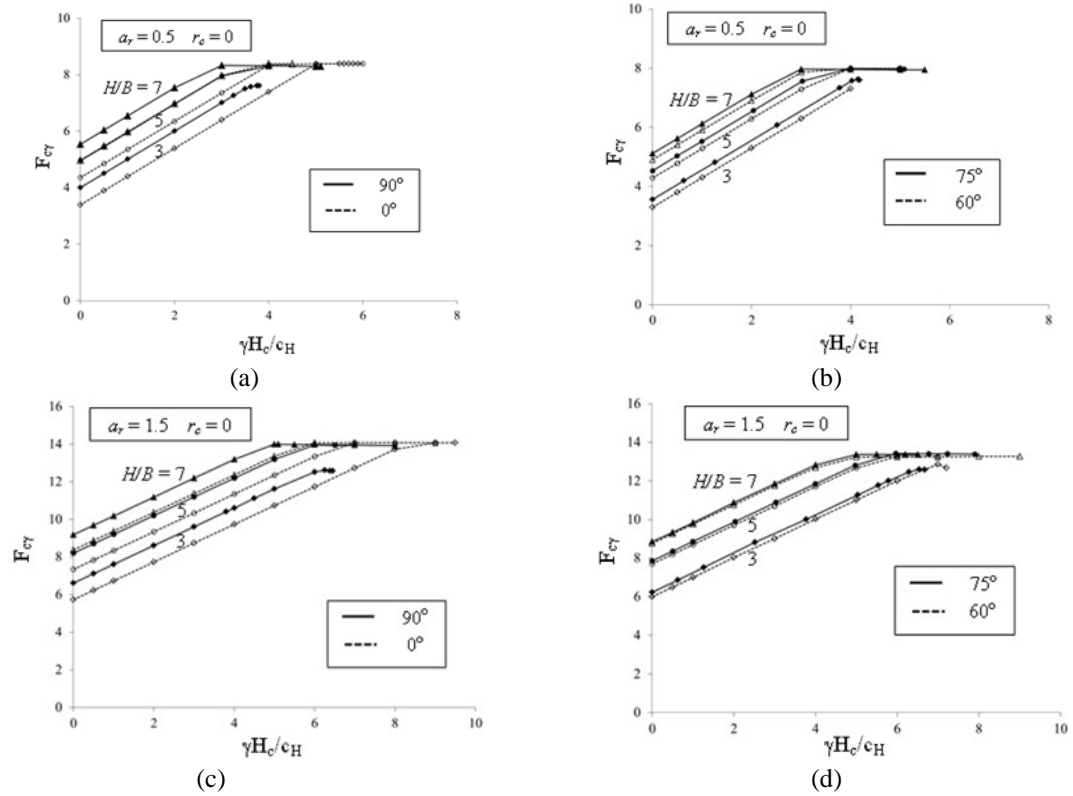


Fig. 11 Variation of $F_{c\gamma}$ with $\gamma H_c/c_u$ for homogeneous anisotropic clay with (a)-(b) $a_r=0.5$ and $r_c=0$ and (c)-(d) $a_r=1.5$ and $r_c=0$

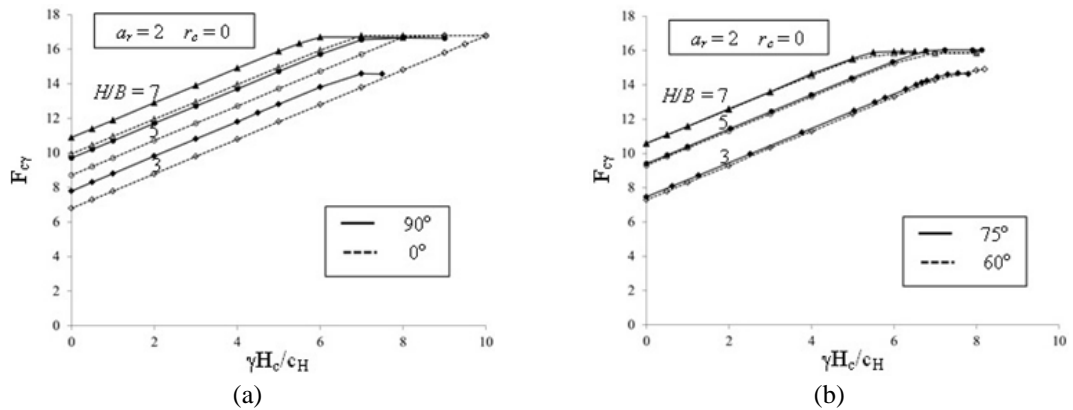


Fig. 12 Variation of $F_{c\gamma}$ with $\gamma H_c/c_u$ for homogeneous anisotropic clay with (a)-(b) $a_r=2$ and $r_c=0$

other inclination angles of the anchor plate which are not shown here. It has been found that a linear relationship exists between the pullout capacity factor ($F_{c\gamma}$) of the anchor plate and the normalized overburden pressure ($\gamma H_c/c_u$) for different inclination of the plate embedded in clay. Similar relationship was also established by Merifield *et al.* (2001) for horizontal and vertical

anchor plates (i.e., $\omega = 0^\circ$ and 90°). However this linear relationship exist up to a critical value of $\gamma H_c/c_u$ i.e., $(\gamma H_c/c_u)_{cr}$ beyond which no change in $F_{c\gamma}$ has been found due to increase in $\gamma H_c/c_u$. In Figs. 10-12 it can be seen that the magnitude of critical value of $\gamma H_c/c_u$ depends on (i) embedment ratio (H/B), (ii) inclination of the anchor plate, (iii) soil anisotropy (in terms of a_r) and (iv) soil non-homogeneity (in terms of r_c). Moreover, at the critical $\gamma H_c/c_u$, the value of $F_{c\gamma}$ has been found to increase due to increase in a_r and decrease in r_c . For any value of $\gamma H_c/c_u$ greater than the critical value of $\gamma H_c/c_u$ the anchor behaves as deep anchor where the failure zone is confined nearby the anchor plate instead of reaching to the ground surface. Since a linear relationship exists between $F_{c\gamma}$ and $\gamma H_c/c_u$ up to the critical value of $\gamma H_c/c_u$ the pullout capacity factor ($F_{c\gamma}$) of shallow anchor late for $\gamma \neq 0$ can be determined by simply adding normalized overburden pressure ($\gamma H_c/c_H$) of the

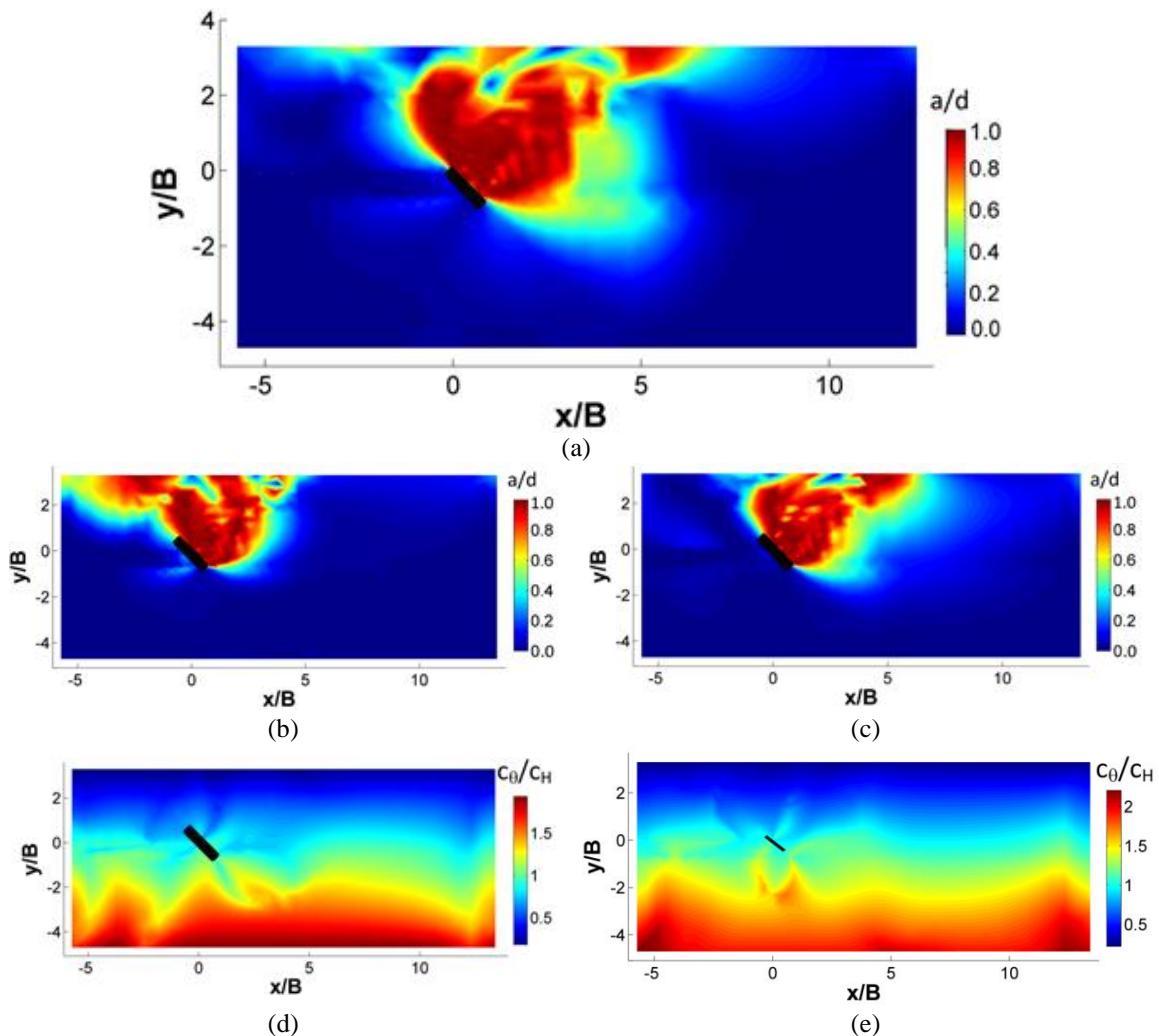


Fig. 13 Proximity of the stress state to failure of anchor plate with $H/B=4$ and $\omega=45^\circ$ for (a) $r_c=0$ and $c_v/c_h=1$, (b) $r_c=1$ and $c_v/c_h=0.5$, (c) $r_c=1$ and $c_v/c_h=1.5$, and (d)-(e) the variation of the cohesion in the soil domain for (d) $r_c=1$ and $c_v/c_h=0.5$ and (e) $r_c=1$ and $c_v/c_h=1.5$

soil mass lying above the anchor plate to the pullout capacity factor F_{c0} as shown below.

$$F_{c\gamma} = F_{c0} + \frac{\gamma H_c}{c_u} \quad (9)$$

4.5 Failure pattern

The proximity of the stress state to shear failure in the optimized statically admissible stress field has been found out in terms of a ratio, a/d , where a and d can be defined as

$$a = (\sigma_y - \sigma_x - 2\tau_{xy} \tan \phi_u)^2 + (c_v - c_h + 2\tau_{xy} - \sigma_x \tan \phi_u + \sigma_y \tan \phi_u)^2$$

$$d = (c_v + c_h - \sigma_x \tan \phi_u - \sigma_y \tan \phi_u)^2$$

The a/d value becomes equal to unity at node subjected to shear failure. The proximity of stress state of soil domain to failure has been shown in Fig. 13 for embedment ratio $H/B = 4$ with $\omega=45^\circ$ for (i) isotropic homogeneous case (refer Fig. 13(a)) and (ii) anisotropic nonhomogeneous cases considering (i) $c_v/c_h=0.5$ and $r_c=1$ and (ii) $c_v/c_h=1.5$ and $r_c=1$ (refer Figs. 13(b)-(c)). In the all cases plastic zone starting from edges of the anchor plate up to the ground surface has been noted on the front side of the plate. The size of the plastic zone has been found to decrease with an increase in the anisotropy cohesion ratio c_v/c_h . The distribution of cohesion in the soil domain for these two cases is also shown in Figs. 13(d)-13(e).

4.6 An example for estimation of pullout capacity of inclined anchor plate in anisotropic nonhomogeneous clay

Table 2 Pullout capacity factor and pullout resistance stress of inclined strip anchor plate with $\omega = 60^\circ$ for different values of H/B and a_r for different values of soil cohesion on the horizontal plane ($r_c = 0$)

H/B	Anisotropic ratio ($a_r=c_v/c_h$)	Pullout capacity factor (F_{c0})		
		Cohesion on horizontal plane (c_h)		
		50 kPa	100 kPa	250 kPa
3	0.5	3.30 (164.86) ^s	3.30 (329.45)	3.30 (823.68)
	1.0	4.70 (234.88)	4.70 (470.42)	4.70 (1174.70)
	1.5	6.01 (300.53)	6.01 (601.08)	4.70 (1502.80)
	2.0	7.29 (364.30)	7.29 (728.51)	7.29 (1821.51)
5	0.5	4.29 (214.30)	4.29 (428.60)	4.29 (1071.53)
	1.0	6.06 (302.83)	6.06 (605.67)	6.06 (1514.13)
	1.5	7.71 (385.51)	7.71 (770.88)	7.71 (1927.20)
	2.0	9.31 (465.33)	9.31 (930.66)	9.31 (2326.64)
7	0.5	4.91 (245.31)	4.91 (490.62)	4.91 (1226.56)
	1.0	6.89 (344.56)	6.89 (689.11)	6.89 (1722.78)
	1.5	8.76 (437.75)	8.76 (875.49)	8.76 (2188.74)
	2.0	10.56 (528.10)	10.56 (1056.14)	10.56 (2640.60)

^sValues reported within bracket are pullout resistance load (kN) for an anchor plate of width $B=1$ m

Table 3 Comparison between pullout resistance load measured directly from the present code to the pullout resistance load measured from Figs. 3-8 and Eq. (10) for anisotropic non-homogeneous clay

Anisotropic ratio (a_r)	Normalized rate of cohesion (r_c)	Pullout capacity (kN) **			Pullout capacity (kN) using Figs. 3-8 and Eq. (10)		
		Cohesion at ground surface			Cohesion at ground surface		
		50 kPa	100 kPa	250 kPa	50 kPa	100 kPa	250 kPa
0.5	0.5	573.55	1147.08	2867.73	572.95	1145.90	2864.74
	1.0	929.11	1858.21	4646.03	927.88	1855.76	4639.40
1.0	0.0[#]	302.88	605.76	1514.40	302.90	605.80	1514.50
	0.5	808.97	1617.92	4044.80	809.13	1618.26	4045.65
	1.0	1309.33	2618.70	6546.65	1309.67	2619.34	6548.35
1.5	0.5	1033.12	2066.23	5165.58	1031.23	2062.46	5156.15
	1.0	1670.43	3340.85	8352.15	1669.90	3339.8	8349.48
2.0	0.5	1248.94	2503.87	6244.67	1246.36	2492.72	6231.80
	1.0	2018.92	4037.80	10094.6	2017.4	4034.79	10085.09

**Width of the anchor plate (B)=1 m

[#]Pullout capacity load (kN) for isotropic homogeneous clay soil with $\gamma=0$

Following procedure can be followed to find the pullout capacity of inclined anchor plate in anisotropic and nonhomogeneous clay:

(i) The shear strength anisotropy of the clay sample can be measured from the laboratory tests. The representative values are c_0 , r_c and c_v/c_h .

(ii) For a particular width of the anchor plate B , embedment ratio H/B and inclination angle of the anchor plate ω the value of H_c can be determined as: $H_c = H - 0.5B \sin \omega$.

(iii) From Table 2, it has been noted that $F_{c0} (F_{c0} = \left(\frac{P_u}{c_h B}\right))$ value will remain unchanged if c_h will change keeping anisotropic ratio a_r same for homogeneous clay ($r_c=0$). Therefore, initially the pullout capacity factor F_{c0} for (i) $c_v/c_h=1$ and $r_c=0$ and (ii) for the required value of c_v/c_h with $r_c=0$ can be determined from Figs. 3-4 depending on the value of ω and H_c/B . If the required c_v/c_h value is not included in Figs. 3-4 then interpolation can be done to obtain F_{c0} . With these two sets of F_{c0} values a ratio α_c equal to $(F_{c0})_{c_v/c_h \neq 1, r_c=0} / (F_{c0})_{c_v/c_h=1, r_c=0}$ can be estimated.

(iv) In next step another ratio η_{rc} as shown in Eq. (8) can be calculated from the two sets of F_{c0} values corresponding to (i) $c_v/c_h=1$ and $r_c \neq 0$ (isotropic but non-homogeneous) and (ii) $c_v/c_h=1$ and $r_c=0$ (isotropic and homogeneous) by using Figs. 5-8.

(v) Finally the pullout capacity factor $(F_{c0})_{c_v/c_h \neq 1, r_c \neq 0}$ (i.e., anisotropic and non-homogeneous clay) for weightless soil can be estimated by using following equation.

$$(F_{c0})_{c_v/c_h \neq 1, r_c \neq 0} = (\alpha_c) (\eta_{rc}) (F_{c0})_{c_v/c_h=1, r_c=0} \tag{10}$$

(vi) Figs. 10-12 represent the linear relationship between pullout capacity factor $F_{c\gamma}$ and $\gamma H_c/c_H$ for shallow anchor (i.e., $\gamma H_c/c_H < (\gamma H_c/c_H)_{cr}$). In order to incorporate the weight of the soil in the pullout capacity of the soil the normalized overburden pressure of the overlying soil ($\gamma H_c/c_H$) will be added to the previous Eq. (10). Hence the pullout capacity factor of shallow anchor plate in soil with finite weight can be determined as

$$(F_{c\gamma})_{c_v/c_h \neq 1, r_c \neq 0} = (F_{c0})_{c_v/c_h \neq 1, r_c \neq 0} + \frac{\gamma H_c}{c_H} \quad (11)$$

However for deep anchor $\gamma H_c/c_H \geq (\gamma H_c/c_H)_{cr}$ instead of using Eq. (11) one may use the maximum value of $(F_{c\gamma})_{c_v/c_h \neq 1, r_c \neq 0}$ for $\gamma H_c/c_H < (\gamma H_c/c_H)_{cr}$ which may provide a slight conservative but safe value for the design.

The validation of the Eq. (11) has been illustrated in Table 3 where maximum difference between pullout capacity ($P_u = F_{c\gamma} A_{plate}$ where A_{plate} is the plan area of the anchor plate) obtained from Eq. (11) and the same obtained by using direct lower bound finite element analysis with coupled non-homogeneous and anisotropic behavior of clay considering all input parameters together is within 1% (most of the cases the difference is below 0.5%).

5. Conclusions

In this article an attempt has been made to calculate the effect of anisotropy and non-homogeneity of clay together on the pullout capacity of the inclined anchor plate by using numerical lower bound finite element analysis. A wide range of inclination angle of the anchor plate has been considered ranging from 0° to 90° with an interval of 15° . The results are presented in terms of variation of pullout capacity factor with normalized embedment depth (H_c/B) considering (i) soil anisotropy and (ii) non-homogeneity separately along with the same for isotropic homogeneous clay. The results clearly indicate that the undrained pullout capacity is greatly influenced by both anisotropic behavior and non-homogeneity of the clay. The pullout capacity of the inclined anchor plate in horizontally strong anisotropic clay has been found to be less compared the pullout capacity of the same inclined anchor plate in isotropy clay. On the other hand, the pullout capacity of the inclined anchor plate in vertically strong anisotropic clay has been found to be higher than the pullout capacity in the isotropic clay. The increase in shear strength with depth induces higher strength in the soil and hence non-homogeneity imparts greater resistance against pullout. The pullout capacity factor decreases with an increase in normalized rate of change in cohesion (r_c) where $r_c > 2$ does not cause a significant reduction in pullout capacity factor (F_{c0}).

References

- Basudhar, P.K. and Singh, D.N. (1994), "A generalized procedure for predicting optimal lower bound break-out factors of strip anchors", *Geotech.*, **44**(2), 307-318.
- Bhattacharya, P. (2016), "Pullout capacity of strip plate anchor in cohesive sloping ground under undrained condition", *Comput. Geotech.*, **78**, 134-143.
- Bhattacharya, P. and Roy, A. (2016), "Improvement in uplift capacity of horizontal circular anchor plate in undrained clay by granular column", *Geomech. Eng.*, **10**(5), 617-633.
- Bishop, A.W. (1966), "The strength of soils as engineering materials", *Géotech.*, **16**, 89-128.
- Bottero, A. Negre, R., Pastor, J. and Turgeman, S. (1980), "Finite element method and limit analysis theory for soil mechanics problem", *Comput. Met. Appl. Mech. Eng.*, **22**(1), 131-149.
- Chen, Z., Tho, K.K., Leung, C.F. and Chow, Y.K. (2013), "Influence of overburden pressure and soil rigidity on uplift behavior of square plate anchor in uniform clay", *Comput. Geotech.*, **52**, 71-81.
- Das, B.M. and Puri, V.K. (1989), "Holding capacity of inclined square plate anchors in clay", *Soils Found.*,

- 29(3), 138-144.
- Das, B.M. and Seeley, G.R. (1975), "Breakout resistance of shallow horizontal anchors", *J. Geotech. Eng. Div.*, **101**(9), 999-1003.
- Davis, E.H. and Christian, J.T. (1971), "Bearing capacity of anisotropic cohesive soil", *J. Soil Mech. Found. Div.*, **97**, 551-563.
- Demir, A. and Ok, B. (2015), "Uplift response of multi-plate helical anchors in cohesive soil", *Geomech. Eng.*, **8**(4), 615-630.
- Desai, C.S., Muqtadir, A. and Scheele, F. (1986), "Interaction analysis of anchor-soil systems", *J. Geotech. Eng.*, **112**(5), 537-553.
- Dickin, E.A. and Leung, C.F. (1983), "Centrifuge model tests on vertical anchor plates", *J. Geotech. Eng.*, **109**(12), 1503-1525.
- Ilamparuthi, K. and Muthukanhaiah, K. (1999), "Anchor in sand bed: Delineation of rupture surface", *Ocean Eng.*, **26**(12), 1249-1273.
- Jha, S.K. (2016), "Reliability-based analysis of bearing capacity of strip footings considering anisotropic correlation of spatially varying undrained shear strength", *J. Geomech.*, **16**(5), 0601003.
- Keskin, M.S. (2015), "Model studies of uplift capacity behaviour of square plate anchors in geogrid-reinforced sand", *Geomech. Eng.*, **8**(4), 595-613.
- Khatri, V.N. and Kumar, J. (2009), "Vertical uplift resistance of circular plate anchors in clays under undrained condition", *Comput. Geotech.*, **36**(8), 1352-1359.
- Kumar, J. and Khatri, V.N. (2008), "Effect of footing width on bearing capacity factor N_f for smooth strip footings", *J. Geotech. Geoenviron. Eng.*, **134**(9), 1299-1310.
- Kupferman, M. (1965), "The vertical holding capacity of marine anchors in clay subjected to static and cyclic loading", MSc. Dissertation, University of Massachusetts, Boston, Massachusetts, U.S.A.
- Lo, K.Y. (1965), "Stability of slopes in anisotropic soils", *J. Soil Mech. Found.*, **91**, 85-106.
- Lyamin, A.V. and Sloan, S.W. (2002), "Lower bound limit analysis using linear finite elements and non-linear programming", *J. Num. Anal. Met. Geomech.*, **55**(5), 573-611.
- Merifield, R.S., Lyamin, A.V. and Sloan, S.W. (2005), "Stability of inclined strip anchor in purely cohesive soil", *J. Geotech. Geoenviron. Eng.*, **131**(6), 792-799.
- Merifield, R.S., Sloan, S.W. and Yu, H.S. (2001), "Stability of plate anchor in undrained clay", *Géotech.*, **51**(2), 141-153.
- Meyerhof, G.G. (1973), "Uplift resistance of inclined anchors and piles", *Proceedings of the 8th International Conference on Soil Mechanics and Foundation*, Moscow, Russia, August.
- Nian, T.K., Chen, G.Q., Luan, M.T., Yang, Q. and Zhang, D.F. (2008), "Limit analysis of the stability of the slopes reinforced with piles against landslide in nonhomogeneous and anisotropic soils", *Can. Geotech. J.*, **45**(8), 1092-1103.
- Niroumand, H. and Kassim, K.A. (2014b), "Experimental and numerical modeling of uplift behavior of rectangular plates in cohesionless soil", *Geomech. Eng.*, **6**(4), 341-358.
- Niroumand, H. and Kassim, K.A. (2014c), "Square plates as symmetrical anchor plates under uplift test in loose sand", *Geomech. Eng.*, **6**(6), 593-612.
- Niroumand, H. and Kassim, K.A. (2014a), "Uplift response of circular plate as symmetrical anchor plates in loose sand", *Geomech. Eng.*, **6**(4), 321-340.
- Ovesen, N.K. (1981), "Centrifuge tests on the uplift capacity of anchors", *Proceedings of the 10th International Conference on Soil Mechanics and Foundation Engineering*, Stockholm, Sweden, June.
- Pan, Q. and Dias, D. (2016), "Face stability analysis for a shield-driven tunnel in anisotropic and nonhomogeneous soils by the kinematical approach", *J. Geomech.*, **16**(3), 04015076.
- Rao, S.N. and Prasad, Y.V.S.N. (1992), "Uplift capacity of plate anchors in sloped clayey ground", *Soils Found.*, **32**(4), 164-170.
- Rowe, R.K. and Davis, E.H. (1982), "The behaviour of anchor plates in clay", *Geotech.*, **32**(1), 9-23.
- Sloan, S.W. (1988), "Lower bound limit analysis using finite elements and linear programming", *J. Num. Anal. Met. Geomech.*, **12**(1), 61-77.

- Song, Z., Yuxia, H. and Randolph, M. (2008), "Numerical simulations of vertical pullout of plate anchors in clay", *J. Geotech. Geoenviron. Eng.*, **134**(6), 866-875.
- Sutherland, H.B. (1988), "Uplift resistance of soils", *Géotech.*, **38**(4), 493-516.
- Tho, K.K., Chen, Z., Leung, C.F. and Chow, Y.K. (2014), "Pullout behaviour of plate anchor in clay with linearly increasing strength", *Can. Geotech. J.*, **51**(1), 92-102.
- Wang, D., Yuxia, H. and Randolph, M. (2010), "Three-dimensional large deformation finite-element analysis of plate anchors in uniform clay", *J. Geotech. Geoenviron. Eng.*, **136**(2), 355-365.
- Yu, H.S. and Sloan, S.W. (1994), "Limit analysis of anisotropic soils using finite elements and linear programming", *Mech. Res. Comm.*, **21**(6), 545-554.
- Yu, H.S. and Wang, J. (2014), "Three-dimensional shakedown solutions for anisotropic cohesive-frictional materials under moving surface loads", *J. Num. Anal. Met. Geomech.*, **38**(4), 331-348.
- Yu, L., Liu, J., Kong, X.J. and Hu, Y. (2011), "Numerical study on plate anchor stability in clay", *Géotech.*, **61**(3), 235-246.
- Yu, S.B., Hambleton, J.P. and Sloan, S.W. (2015), "Undrained uplift capacity of deeply embedded strip anchors in non-uniform soil", *Comput. Geotech.*, **70**, 41-49.
- Yu, S.B., Merifield, R.S., Lyamin, A.V. and Fu, X.D. (2014), "Kinematic limit analysis of pullout capacity for plate anchors in sandy slopes", *Struct. Eng. Mech.*, **51**(4), 565-579.